Numerical modeling of ductile porous material with a general plastic matrix

Long CHENG[a], Stella BRACH[b], Albert GIRAUD[a], Dijmédo KONDO[c]

a. Université de Lorrain, GeoRessources, UMR 7359 CNRS, long.cheng@univ-lorraine.fr, albert.giraud@univ-lorraine.fr

b.Division of Engineering and Applied Science, California Institute of Technology, 1200 E California Blvd, Pasadena, CA 91125 - États-Unis, brach@caltech.edu

c. Institut Jean Le Rond d'Alembert, UMR CNRS 7190 Sorbonne Université, djimedo.kondo@upmc.fr

Résumé :

Cette étude vise à proposer une méthode numérique afin d'estimer la réponse macroscopique pour des milieux poreux ductiles dont la matrice obéit à un critère isotrope de plasticité dépendant des trois invariants du tenseur de contrainte. A cette fin, le critère général initialement proposé par Bigoni et al.,(2004)[2] et récemment particularisé par Brach et al., (2017) [3] est considéré. Ceci permet de disposer d'un cadre unifié pour la détermination des charges limites pour une large classe de matériaux incluant les métaux, les géomatériaux et les polymères qui sont eux sensibles à la pression, etc. Plus précisément, une procédure basée sur la méthode d'éléments finis est mis en œuvre pour calculer les surfaces de plasticité macroscopiques pour divers types de matériaux poreux. Ceci nous a permis d'évaluer divers modèles théoriques en portant une attention particulière à l'effet de l'angle de Lode de la matrice. Les prédictions de la modélisation numérique proposée sont également confirmées et validées en les comparant avec des bornes supérieures et inférieures numériques disponibles dans littérature.

Abstract :

The aim of this work is to propose a numerical estimate of the macroscopic response for ductile porous material by considering the local plastic behavior as dependent on all the three isotropic stress invariants. In this light, the general and flexible yield criterion proposed by Bigoni et al., 2004 [2] and recently particularized by Brach et al., 2017 [3] is considered as a promising candidate to comply with benchmarking indications on local strength properties. This allows to effectively describe the limit behavior of a broad class of materials, such as pressure independent metals, pressure sensitive geomaterials and polymers, high strength shape memory alloys, etc. Specifically, a Finite Element-based limit analysis procedure is implemented in order to compute the macroscopic yield surfaces. This allows to assess theoretical predictions and study different type of porous materials and structures by paying particular attention to the matrix Lode angle effects. The proposed numerical model is assessed and validated by comparing its predictions with the available upper and lower bounds in literature.

Mots clefs : Numerical homogenization ; limit analysis ; porous material ; general plastic model ; Lode angle effect

1 Introduction

Micromechanical investigation of porous materials starts about fifty years ago with studies by McClintock [10] and Rice and Tracy [12] based on variational procedures. They have been developed for ductile porous materials that do not account for any coupling between the plasticity of the matrix materials and the void growth. Coupled models has been initiated by Gurson [7] who has proposed in his famous paper an upper bound limit analysis approach by using simplify microstructures such as the hollow sphere and hollow cylinder having a von Mises solid matrix. Several extensions of Gurson model have been further developed in literature that account for the void shape effects and traction-compression asymmetry, etc. Considering the micromechanical modeling for applications to cohesive materials (e.g. geomaterials, polymers, etc.), Guo et al., 2008 [8] and Cheng et al., 2015 [5] have both adopted the theoretical and numerical homogenization to take into account the plastic compressibility of the matrix respectively obeying the associated and non-associated Drucker-Prager yielding laws. However, the aforementioned models have been derived by assuming that the solid matrix obeys a yield criterion either depending on the second stress invariant (i.e. J2 plastic rule) or accounting for the first and the second ones. Nevertheless, the solid matrix of some engineering-relevant porous materials may exhibit a more complex plastic behavior that also depends on the third stress invariant, that is on the stress-Lode-angle. Few attempts have been made in literature to include the influence of all the three isotropic stress invariants for describing strength properties of porous media. Mention can be made of the studies by Lemarchand et al., 2015 [9], Anoukou et al., 2016 [1], Pastor et al., 2016 [11]. Some of these studied have been devoted to the special case of Mohr-Coulomb plastic matrix.

Let us now come to a more general point of view, Brach et al. [3] has proposed a modified form of strength criterion based on the one of [2] allowing a versatile description of the three isotropic stress invariants dependence. Concerning porous materials with such a general plastic matrix, mention has to be made of the theoretical homogenization procedure recently carried out in [4]. The objective of the present study is to propose a numerical tool able to provide estimates of the macroscopic limit state for porous materials with a general plastic matrix. To this end, the yield criterion established in [3] is adopted and implemented for the Finite Elements based homogenization and limit analysis.

2 Constitutive relation of general elasto-perfect-plasticity

We describe in this section the constitutive relation for the matrix material of the porous media, which is considered to obey a general elasto-perfectly-plastic law. Considering that the matrix as well as the porous material are both under small strains conditions, the microscopic strain rate tensor $\boldsymbol{d}$ can be classically decomposed in the form :

$$\boldsymbol{d} = \boldsymbol{d}^e + \boldsymbol{d}^p \tag{1}$$

where $\boldsymbol{d}^e$ and $\boldsymbol{d}^p$ are respectively its elastic and plastic parts.

By applying the Hooke's law, one has

$$\boldsymbol{d}^e = \mathbb{M} : \dot{\boldsymbol{\sigma}} = \mathbb{L}^{-1} : \dot{\boldsymbol{\sigma}}, \quad \text{with} \quad \mathbb{M} = \frac{1}{2\mu_e}\mathbb{K} + \frac{1}{3\kappa_e}\mathbb{J} \quad \text{and} \quad \mathbb{L} = 2\mu_e\mathbb{K} + 3\kappa_e\mathbb{J} \tag{2}$$

where $\boldsymbol{\sigma}$ is the microscopic Cauchy stress tensor, $\mathbb{M}$ and $\mathbb{L}$ respectively denote the elastic compliance tensor and stiffness tensor which, due to the isotropy, depend on the elastic shear and bulk moduli μ_e and κ_e.

Still, in isotropic case, the plastic limit stress state of the matrix can be fully defined by means of the microscopic mean stress (or hydrostatic) σ_m, equivalent stress σ_{eq} and stress Lode angle $\theta^{\boldsymbol{\sigma}}$:

$$\sigma_m = \frac{I_1^{\boldsymbol{\sigma}}}{3}, \quad \sigma_{eq} = \sqrt{3J_2^{\boldsymbol{\sigma}}}, \quad \cos(3\theta^{\boldsymbol{\sigma}}) = \frac{3\sqrt{3}}{2}\frac{J_3^{\boldsymbol{\sigma}}}{(J_2^{\boldsymbol{\sigma}})^{3/2}} \tag{3}$$

where $I_1^{\boldsymbol{\sigma}} = \mathrm{tr}(\boldsymbol{\sigma})$, $J_2^{\boldsymbol{\sigma}} = \mathrm{tr}(\boldsymbol{\sigma}_d^2)/2$ and $J_3^{\boldsymbol{\sigma}} = \mathrm{tr}(\boldsymbol{\sigma}_d^3)/3$ are respectively the first invariant of the microscopic stress tensor $\boldsymbol{\sigma}$, the second and third invariants of the microscopic stress deviator $\boldsymbol{\sigma}_d = \boldsymbol{\sigma} - \sigma_m \mathbf{1}$.

Following [3], the local plastic criterion is defined as

$$\mathcal{G}^s(\boldsymbol{\sigma}) = m(\boldsymbol{\sigma}) + \frac{\sigma_{eq}}{g(\boldsymbol{\sigma})}, \quad m(\boldsymbol{\sigma}) = -3(h - \frac{\sigma_m}{\xi}), \quad g(\boldsymbol{\sigma}) = \frac{1}{\cos\left[\frac{\pi}{6}\beta - \frac{1}{3}\cos^{-1}(\gamma\cos(3\theta^{\boldsymbol{\sigma}}))\right]} \tag{4}$$

where the scalar function $m(\boldsymbol{\sigma})$ and $g(\boldsymbol{\sigma})$ define the plastic yield profile respectively in meridian plane (i.e. $\sigma_{eq} = $ const.) and deviatoric one (i.e. $\sigma_{eq} = $ const.) [3, 2]. Note that in Eq.(4), h, ξ, β and γ are four material parameters. More specifically h and ξ are positive defined for physical admissibility reason, β and γ being dimensionless material parameters which requires the consistency conditions $0 \leq \beta \leq 2$ and $0 \leq \gamma \leq 1$ to guarantee the convexity of the yield function in the local stress π plane. The parameter γ induces a smoothing effect on corners.

Next, considering the associated plasticity in the present work, the microscopic plastic strain rate $\boldsymbol{d}^p$ can be calculated by applying the normality law :

$$\boldsymbol{d}^p = \dot{\lambda}\frac{\partial \mathcal{P}^s}{\partial \boldsymbol{\sigma}} \tag{5}$$

By combining Eqs.(1), (5) and (2), one has

$$\dot{\boldsymbol{\sigma}} = \mathbb{L} : \left(\boldsymbol{d} - \dot{\lambda}\frac{\partial \mathcal{G}^s(\boldsymbol{\sigma})}{\partial \boldsymbol{\sigma}}\right) \tag{6}$$

with the plastic multiplier $\dot{\lambda}$.
Since the yield function is isotropic and rate-independent, the consistency condition can be written in the following form :

$$\dot{\mathcal{G}}^s(\boldsymbol{\sigma}) = \frac{\partial \mathcal{G}^s(\boldsymbol{\sigma})}{\partial \boldsymbol{\sigma}} : \dot{\boldsymbol{\sigma}} = 0 \tag{7}$$

Inserting Eqs.(6) into (7), one has

$$\dot{\lambda} = \frac{\frac{\partial \mathcal{G}^s(\boldsymbol{\sigma})}{\partial \boldsymbol{\sigma}} : \mathbb{L} : \boldsymbol{d}}{\frac{\partial \mathcal{G}^s(\boldsymbol{\sigma})}{\partial \boldsymbol{\sigma}} : \mathbb{L} : \frac{\partial \mathcal{G}^s(\boldsymbol{\sigma})}{\partial \boldsymbol{\sigma}}} \tag{8}$$

The rate form of the elasto-perfect-plastic constitutive relation Eq.(6) can be explicitly expressed as

$$\dot{\boldsymbol{\sigma}} = \mathbb{L}^{ep} : \boldsymbol{d}, \quad \text{with} \quad \mathbb{L}^{ep} = \mathbb{L} - \frac{\left(\mathbb{L} : \frac{\partial \mathcal{G}^s(\boldsymbol{\sigma})}{\partial \boldsymbol{\sigma}}\right) \otimes \left(\frac{\partial \mathcal{G}^s(\boldsymbol{\sigma})}{\partial \boldsymbol{\sigma}} : \mathbb{L}\right)}{\frac{\partial \mathcal{G}^s(\boldsymbol{\sigma})}{\partial \boldsymbol{\sigma}} : \mathbb{L} : \frac{\partial \mathcal{G}^s(\boldsymbol{\sigma})}{\partial \boldsymbol{\sigma}}} \tag{9}$$

3 Numerical homogenization

We consider an axisymmetric hollow sphere Ω in the macroscopic cylindrical coordinates $(\boldsymbol{e}_\rho, \boldsymbol{e}_\varphi, \boldsymbol{e}_z)$ composed of a void ω embedded in a rigid perfectly plastic matrix $\Omega_M = \Omega - \omega$. The external and internal boundaries of the hollow sphere Ω are respectively denoted by $\partial\Omega$ and $\partial\omega$. The hollow sphere is subjected to a velocity boundary condition on the external surface $\partial\Omega$ given by $\boldsymbol{v} = \boldsymbol{D} \cdot \boldsymbol{x}$ with $\boldsymbol{D}$ being the macroscopic strain rate and $\boldsymbol{x}$ denoting the position vector at $\partial\Omega$. In the frame work of homogenization, the macroscopic stress $\boldsymbol{\Sigma}$ and strain rate $\boldsymbol{D}$ can then be classically defined as volume averages of their microscopic counterparts $\boldsymbol{\sigma}$ and $\boldsymbol{d}$:

$$\begin{aligned} \boldsymbol{\Sigma} &= \frac{1}{\mid \Omega \mid} \int_\Omega \boldsymbol{\sigma} \, dV = \Sigma_\rho (\boldsymbol{e}_\rho \otimes \boldsymbol{e}_\rho + \boldsymbol{e}_\varphi \otimes \boldsymbol{e}_\varphi) + \Sigma_z \boldsymbol{e}_z \otimes \boldsymbol{e}_z \\ \boldsymbol{D} &= \frac{1}{\mid \Omega \mid} \int_\Omega \boldsymbol{d} \, dV = D_\rho (\boldsymbol{e}_\rho \otimes \boldsymbol{e}_\rho + \boldsymbol{e}_\varphi \otimes \boldsymbol{e}_\varphi) + D_z \boldsymbol{e}_z \otimes \boldsymbol{e}_z \end{aligned} \tag{10}$$

Hence, the macroscopic mean stress Σ_m, equivalent stress Σ_{eq} and the stress Lode angle $\theta_{\boldsymbol{\Sigma}}$ can be calculated as :

$$\Sigma_m = \frac{2\Sigma_\rho + \Sigma_z}{3}, \quad \Sigma_{eq} = \mid \Sigma_\rho - \Sigma_z \mid, \quad \cos(3\theta_{\boldsymbol{\Sigma}}) = \text{sign}(J_3^{\boldsymbol{\Sigma}}) \quad (\text{i.e. } \theta_{\boldsymbol{\Sigma}} = 0 \text{ or } \frac{\pi}{3}) \tag{11}$$

with $J_3^{\boldsymbol{\Sigma}} = \text{tr}(\boldsymbol{\Sigma}_d^3)/3$ is the third invariants of the macroscopic stress deviator $\boldsymbol{\Sigma}_d = \boldsymbol{\Sigma} - \Sigma_m \mathbf{1}$.
Similarly, the macroscopic strain rate can be represented by :

$$D_m = \frac{2D_\rho + D_z}{3}, \quad D_{eq} = \frac{2}{3} \mid D_\rho - D_z \mid, \quad \cos(3\theta_{\boldsymbol{D}}) = \text{sign}(J_3^{\boldsymbol{D}}) \quad (\text{i.e. } \theta_{\boldsymbol{D}} = 0 \text{ or } \frac{\pi}{3}) \tag{12}$$

where $I_1^{\boldsymbol{D}} = \text{tr}(\boldsymbol{D})$, $J_2^{\boldsymbol{D}} = \text{tr}(\boldsymbol{D}_d^2)/2$ and $J_3^{\boldsymbol{D}} = \text{tr}(\boldsymbol{D}_d^3)/3$ with $\boldsymbol{D}_d = \boldsymbol{D} - D_m \mathbf{1}$ being the macroscopic strain rate deviator.
Moreover, we define the scalar macroscopic deviatoric stress Σ_{gps} in relation with the sign of the macroscopic third stress invariant $J_3^{\boldsymbol{\Sigma}}$ (i.e. $\theta_{\boldsymbol{\Sigma}}$) through :

$$\Sigma_{gps} = \Sigma_\rho - \Sigma_z = -\text{sign}(J_3^{\boldsymbol{\Sigma}}) \Sigma_{eq} \tag{13}$$

Note that the subscript representing the boundary condition of the hollow sphere under macroscopic generalized plane strain-rate [1].

3.1 Implementation of the matrix constitutive model

The general elasto-perfectly plastic constitutive relation obtained in section 2 is implemented into an Umat subroutine (User defined material) by adopting the software Abaqus. Specifically, for each Gauss point, we have, at the beginning of increment $t = t_n$, the known quantities $\boldsymbol{\sigma}_n$, $\boldsymbol{\varepsilon}_n$, $\triangle\boldsymbol{\varepsilon}_n$, $\boldsymbol{\varepsilon}_n^p$, while at the end of the increment $t = t_{n+1}$, $\boldsymbol{\sigma}_{n+1}$, $\boldsymbol{\varepsilon}_{n+1}^p$ should be calculated and updated.
Next, by defining the standard "elastic predictor" $\boldsymbol{\sigma}^e = \boldsymbol{\sigma}_n + \mathbb{L} : \triangle\boldsymbol{\varepsilon}_n$, we have

- during the elastic loading (i.e. $\mathcal{G}^s(\boldsymbol{\sigma}^e) < 0$) : $\boldsymbol{\sigma}_{n+1} = \boldsymbol{\sigma}^e$ and $\boldsymbol{\varepsilon}_{n+1}^p = \mathbf{0}$
- during the plastic loading (i.e. $\mathcal{G}^s(\boldsymbol{\sigma}^e) \geq 0$) : $\boldsymbol{\sigma}_{n+1} = \boldsymbol{\sigma}^e + \triangle\boldsymbol{\sigma}$ and $\boldsymbol{\varepsilon}_{n+1}^p = \boldsymbol{\varepsilon}_n^p + \triangle\lambda \cdot \frac{\partial \mathcal{P}^s}{\partial \boldsymbol{\sigma}_n} \mid_n$

The plastic multiplier $\triangle\lambda$ as well as the stress correction $\triangle\boldsymbol{\sigma}$ can be calculated by using an implicit Newton-Raphson scheme by solving the following equations :

$$\begin{aligned} &\mathcal{G}^s(\boldsymbol{\sigma}^e + \triangle\boldsymbol{\sigma}_n) = 0 \\ &\triangle\boldsymbol{\sigma}_n - \mathbb{L} : \triangle\boldsymbol{\varepsilon}_n + \triangle\lambda\mathbb{L} : \frac{\partial\mathcal{P}^s}{\partial\boldsymbol{\sigma}_n} \mid_n = \mathbf{0} \end{aligned} \quad (14)$$

Note that in the present work, the local plastic singularities in the case of $\gamma = 1$ upon the deviatoric stress π plane can be automatically regularized by adopting a relatively approximate value, for instance $\gamma = 0.99$. This approximation will show to be sufficiently accurate and efficient in the numerical simulations.

3.2 Multipoints constraint boundary conditions

As aforementioned, any macroscopic loading applied to the axsymmetric hollow sphere can be referred to one of two following cases in relation with the macroscopic stress triaxiality T. Let us denote in cylindrical coordinates :

— Axisymmetric extension (denoted AE) :

$$\text{sign}(J_3^{\boldsymbol{\Sigma}}) > 0 \quad \text{and} \quad \theta_{\boldsymbol{\Sigma}} = 0: \quad \Sigma_z \geq \Sigma_\rho = \Sigma_\varphi \quad (15)$$

T is then expressed as $T = \frac{1+2\tau}{3(1-\tau)}$ with $\tau = \Sigma_\rho/\Sigma_z$

— Axisymmetric compression (denoted AC) :

$$\text{sign}(J_3^{\boldsymbol{\Sigma}}) < 0 \quad \text{and} \quad \theta_{\boldsymbol{\Sigma}} = \frac{\pi}{3}: \quad \Sigma_\rho = \Sigma_\varphi \geq \Sigma_z \quad (16)$$

T can be recast into $T = \frac{2+\varsigma}{3(1-\varsigma)}$ with $\varsigma = \Sigma_z/\Sigma_\rho$

The numerical homogenization will then be carried out by developing and implementing a user-defined subroutine called Multi-Points Constraints (MPCs) of Abaqus. It is used, for instance, to describe the velocity field $\boldsymbol{v}$ on the external boundary of the hollow sphere such that the constraint of constant macroscopic stress triaxiality T can be always fulfilled during the elasto-plastic loading :

$$\boldsymbol{v} = \boldsymbol{D}(\tau, \varsigma) \cdot \boldsymbol{x} \quad \mapsto \quad v_\rho = D_\rho(\tau, \varsigma) \cdot x_\rho, \quad v_z = D_z(\tau, \varsigma) \cdot x_z \quad (17)$$

with $\boldsymbol{x} = x_\rho \boldsymbol{e}_\rho + x_\theta \boldsymbol{e}_\theta + x_z \boldsymbol{e}_z$ the position vector in cylindrical coordinates of any point of the external boundary of the hollow sphere. Readers are referred to [5, 6] for more details about the MPCs boundary conditions.

4 Illustration, assessment and validation

We first present in Fig.1 an example of results obtained frome computations performed in the case of porosity $f = 10\%$. The material parameters $h = 0.5323$, $\xi = 5.1620$, $\beta = 0.6277$ and $\gamma = 1$ correspond to a Mohr-Coulomb type matrix : friction angle $\phi = 20°$ and cohesion $c = 1MPa$. We compare the obtained results to the analytical model proposed by [1] and to the numerical limit analysis (upper and lower bounds) from [11]. Excellent agreement is noted, especially between the numerical homogenization results and the upper and lower bounds. It is also worthy to note that the slight difference between them may be due to the approximation adopted in the treatment of the yield singularities in the deviatoric plane. Next, Fig.2 illustrates in general cases the effect of ξ, β and γ on the macroscopic strength surface. Specifically, it can be observed in Fig.2(a) that the asymmetry between the traction

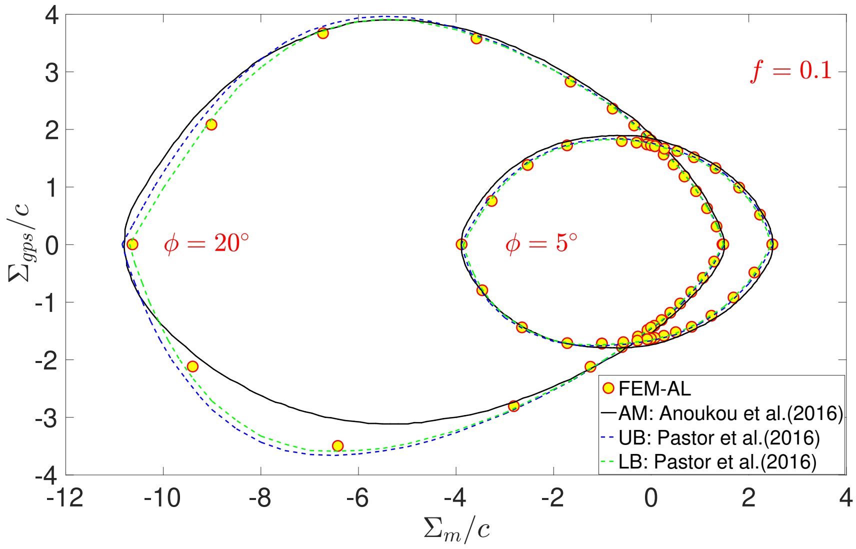

FIGURE 1 – Assessment and validation of the numerical homogenization model proposed in the present study (denote FEM) by comparing its prediction with the numerical upper and lower bounds (respectively denoted UB and LB) of [11] and the analytical macroscopic yield criterion (denoted AM) proposed by [1] in the associated Mohr-Coulomb case for porosity $f = 0.1$ and friction angle $\phi = 20°$ and $5°$.

($\Sigma_m > 0$) and compression ($\Sigma_m < 0$) increases with the decreasing of ξ value, while the one between AE ($J_3^{\boldsymbol{\Sigma}} > 0$) and AC ($J_3^{\boldsymbol{\Sigma}} < 0$) is less important. Moreover, as illustrated in Fig.2(c), the asymmetry between traction and compression is less important when γ varies, whereas the AE-AC asymmetry is significant when $\gamma = 1$ (i.e. Mohr-Coulomb type matrix) which is due to the "extremely" effect of the microscopic Lode angle effect. Finally, it is interesting to note, by comparing Fig.2(b) with 2(a) and 2(c), that the parameter β has both important influence on the macroscopic traction-compression asymmetry and on the AE-AC one. It is logical since that this parameter β could substantially change the local plastic yield loci not only on the meridian plane but also on the deviatoric one (see Eq.(4)). Consequently, the macroscopic yield strength has a relatively significant sensitivity on it after homogenization.

5 Conclusion

In this work, we have developed a finite elements based micromechanical modeling approach of the limit state of porous media with a general plastic matrix. The local behavior is described by the plastic strength criterion proposed in [3] which is implemented in a UMAT subroutine. The numerical homogenization has been performed by defining a macroscopic stress third invariant sign dependent Multi-Points Constraints boundary conditions. We demonstrate the capability of the resulting numerical model to produce very accurate estimates of the macroscopic yield surfaces, validated here by comparaison to available numerical limit analysis bounds. Note that, although the implemented model is used here only for limit analysis purpose, the numerical tool can be also used for various structural computations involving materials which can be suitably described by the developed general model.

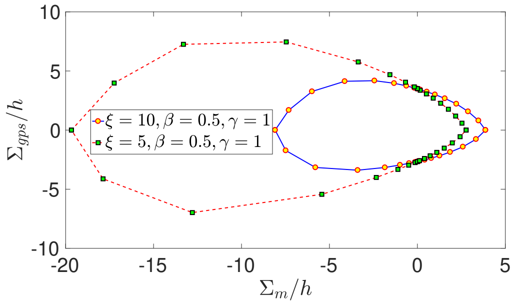

(a) Effect of ξ

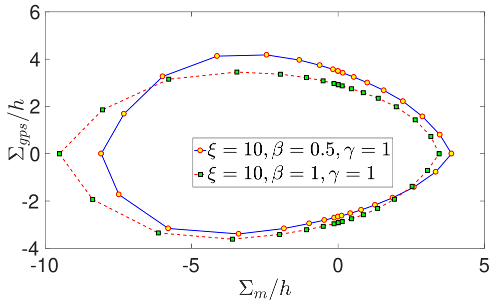

(b) Effect of β

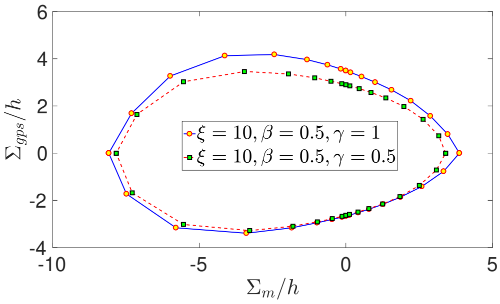

(c) Effect of γ

FIGURE 2 – Effect of material parameter ξ, β and γ on macroscopic yield surface.

Références

[1] Anoukou, K., Pastor, F., Dufrenoy, P., Kondo, D., Limit analysis and homogenization of porous materials with Mohr–Coulomb matrix. Part I : theoretical for- mulation. J. Mech. Phys. Solids, 91(2016), 145–171.

[2] Bigoni, D., Piccolroaz, A., Yield criteria for quasibrittle and frictional materials. Int. J. Solids Struct. 41(2004), 2855-2878.

[3] Brach, S., Dormieux, L., Kondo, D., Vairo G., 2017. Nanoporous materials with a general isotropic plastic matrix : Exact limit state under isotropic loadings. International Journal of Plasticity, 89, 1-28.

[4] Brach, S., Dormieux, L., Kondo, D., Vairo G., Nanoporous materials with a general isotropic plastic matrix : Exact limit state under isotropic loadings. International Journal of Plasticity, 89(2018), 1-28.

[5] Cheng, L., Jia. Y., Oueslati, A., de Saxcé, G., Kondo, D., A bipotential-based limit analysis and homogenization of ductile porous materials with non-associated Drucker–Prager matrix. J. Mech. Phys. Solids, 77 (2015), 1-26.

[6] Micromechanical modeling of porous material with a general isotropic plastic matrix by numerical method. Under submission.

[7] Gurson, A.L., 1977. Continuum theory of ductile rupture by void nucleation and growth. J. Engng. Mater.

[8] Guo, T.F., Faleskog, J., Shih, C.F., 2008. Continuum modeling of a porous solid with pressure-sensitive dilatant matrix. J. Mech. Phys. Solids 56, 2–15.

[9] Lemarchand, E., Dormieux, L., Kondo, D., 2015 Lode's angle effect on the definition of the strength criterion of porous media. International Journal for Numerical and Analytical Methods in Geomechanics, Wiley, 2015, 39 (14), pp.1506–1526.

[10] McClintock, F.A., 1968. A criterion for ductile fracture by the growth of holes. Journal of Applied Mechanics, Vol.35, 363-371.

[11] Pastor, J.F., Anoukou, K., Pastor, J., Kondo, D., 2016. Limit analysis and homogenization of porous materials with Mohr-Coulomb matrix. Part II : numerical bounds and assessment of the theoretical model. J. Mech. Phys. Solids 91, 14–27.

[12] Rice, J.R. and Tracey, D.M., 1969. On the ductile fracture enlargement of voids in triaxial stress fields. J.Mech. Phy. Solids, Vol.17, 201-217.